

ACCELERATION PERFORMANCE OF THE INS 25.5-MHZ SPLIT COAXIAL RFQ

N. Tokuda, S. Arai, A. Imanishi, T. Morimoto, S. Shibuya*, and E. Tojyo
 Institute for Nuclear Study, University of Tokyo
 Tanashi, Tokyo 188, Japan

Abstract

The INS 25.5-MHz split coaxial RFQ, which accelerates ions with a charge-to-mass ratio greater than 1/30 from 1 to 45.4 keV/u, is now taking acceleration tests with a beam of N_2^+ , N^+ , and Ne^+ ions. The electrodes are modulated vanes machined by means of the two-dimensionally cutting technique; consequently, the transverse radius of curvature at the vane tip is constant. Measured emittances and energy spectra of the output beam agree fairly well with the PARMTEQ simulation. The transmission efficiency data show that, in the beam bunching process, the longitudinal electric field is weaker than that derived from the two-term potential function but closer to that numerically computed by Crandall.

Introduction

The INS 25.5-MHz split coaxial RFQ is a linac that accelerates heavy ions with a charge-to-mass ratio greater than 1/30 from 1 up to 45.4 keV/u. The RFQ, 2.1 m in length and 0.90 m in inner diameter, has a multi-module structure: the whole cavity consists of three cavities. We use modulated vanes to generate the electric field for the acceleration and focusing. The cavity structure and its rf characteristics were reported elsewhere^{1,2}.

The RFQ has been undergoing acceleration tests since the first acceleration in January, 1991. The main issue of the tests is to examine the performance of the modulated vanes that were machined by means of the two-dimensional cutting technique without correcting the A_{10} coefficient. The A_{10} term is the principal term of the longitudinal component of the electric field expanded into a Fourier-Bessel series. At the design of the RFQ, we used the PARMTEQ program, assuming A_{10} to be equal to A , the A_{10} coefficient for the ideal vanes, whose surfaces are same as equipotential surfaces defined by the two-term potential function³. According to Crandall's computation⁴, however, A_{10} is smaller than A during the beam bunching process in our RFQ with two-dimensionally

cut vanes. We hence expect this affects the acceleration performance of the RFQ. In the previous paper⁵, we showed experimental data of the output beam current as a function of the intervane voltage, and mentioned that the data indicated the A_{10} effect. At that time, however, we had not enough data for the discussion on the A_{10} problem, because we had no ion-separating device in the low-energy beam transport line and therefore could not measure the transmission efficiency. After improving the beam transport, we have accumulated data of the transmission efficiency as a function of the intervane voltage and can now discuss the problem.

In this paper, we describe the improvement of the acceleration test stand, show some results of experiments, and discuss the A_{10} problem.

Acceleration Test Stand

The acceleration test stand is shown in Fig. 1. The test stand previously reported⁵ has been improved as follows. The low-energy beam transport line is now equipped with an electrostatic steering deflector and an ion separator, a magnet bending the beam by 22.5° in the vertical plane. In the high-energy beam transport line, an additional Faraday cup (Faraday Cup 3) was set in front of the momentum-analyzing magnet. The new device is for the convenience of measuring the current of accelerated ions. At the current measurement, we excite the quadrupole magnets so as to guide the accelerated ions into the Faraday cup and sweep away unaccelerated drift-through ions. With small emittances, however, some of the unaccelerated ions would reach the Faraday cup. By means of a computer simulation, we estimate the amount of such unwanted ions and correct the measured current.

The ions used in acceleration tests are N_2^+ , N^+ , and Ne^+ , which are produced in a 2.86-GHz ECR ion source⁶. The peak current of the beam is in the order of 0.1 mA. The RFQ is operated with a repetition rate of 50 Hz and a duty factor of 2 ~ 5%. The width of the beam pulse is about a half of the rf pulse width.

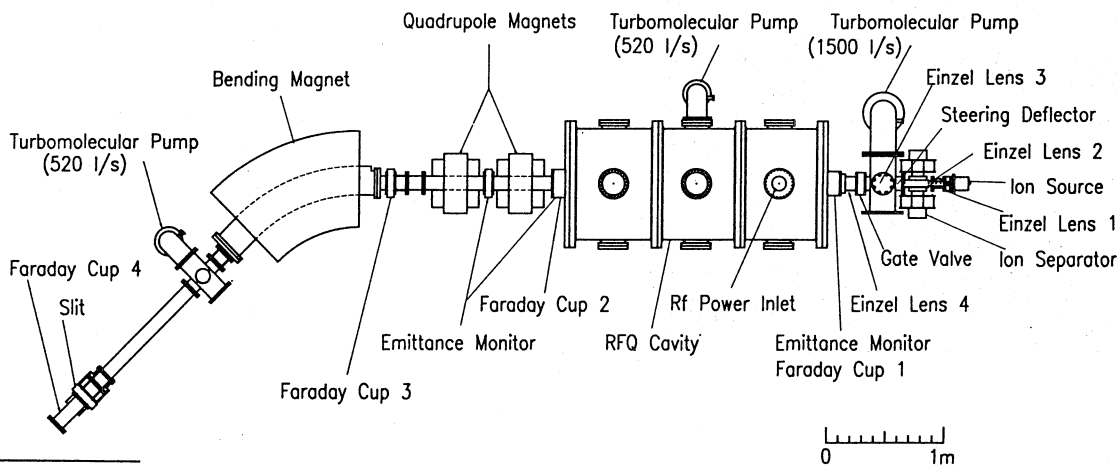


Figure 1. Layout of the acceleration test stand.

*The Graduate University for Advanced Studies, KEK, Tsukuba, Ibaraki 305, Japan

Acceleration Test Results

Emittance

Figure 2 shows emittance profiles at the entrance of the RFQ. The ellipses are the emittances matching to the RFQ acceptance. The ellipse area is $411 \pi \text{ mm}\cdot\text{mrad}$ ($0.6 \pi \text{ mm}\cdot\text{mrad}$ normalized). The bars indicate measured profiles of N^+ ions. These profiles are the ones after cutting off tails at a threshold level, 10% of the maximum density.

At the exit of the RFQ, the above N^+ beam has the emittances shown in Fig. 3, where V_n is the intervine voltage normalized by the design value, 51 kV for N^+ . The dots indicate results of a PARMTEQ simulation, where the input emittances are shaped to ellipses approximately same as the measured profiles in Fig. 2. The measured output emittances are not consistent with the input ones. At the horizontal plane, the input beam is on the beam axis, but the center of the output beam moves as the intervine voltage changes. At the vertical plane, the input beam is off the axis, but the output beam stays on the axis. This inconsistency could be attributed to inaccuracy in the measurement of the input-beam emittance rather than to imperfection in the RFQ.

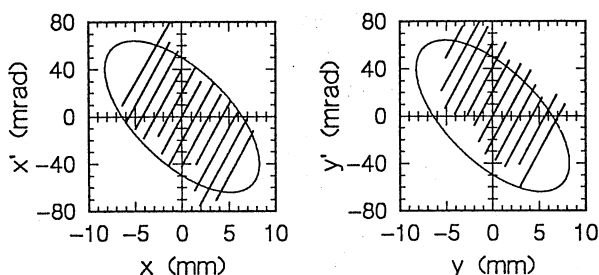


Figure 2. Horizontal (left) and vertical (right) emittance profiles of N^+ ions at the entrance of the RFQ. The bars indicate measured profiles, and the ellipses the designed emittances matching to the RFQ acceptance ($\epsilon_n = 0.6 \pi \text{ mm}\cdot\text{mrad}$).

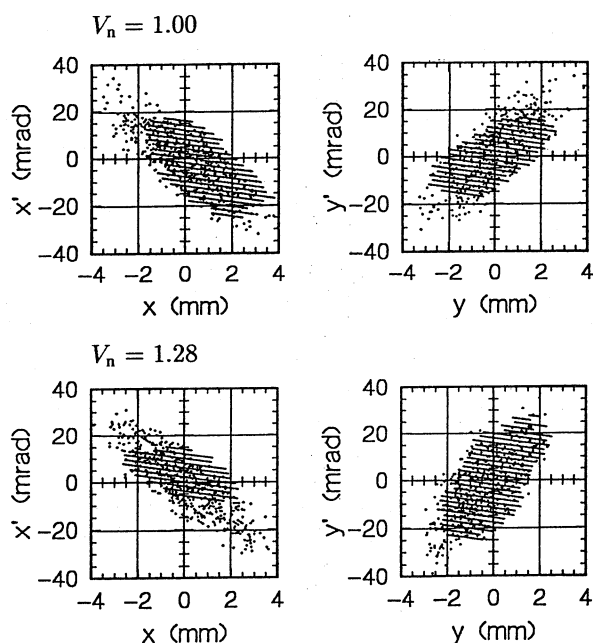


Figure 3. Emittance profiles of N^+ ions at the exit of the RFQ, operated at $V_n = 1$ (top) and 1.28 (bottom). The bars indicate measured profiles, and the dots PARMTEQ simulation results.

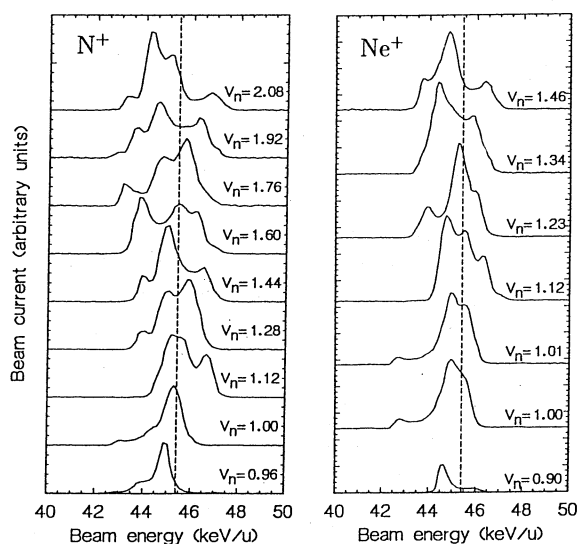


Figure 4. Energy spectra of N^+ and Ne^+ ions for several values of the normalized intervine voltage V_n . The dashed lines indicate the design energy of 45.4 keV/u.

Energy spectra

Energy spectra of the output beam were measured at various values of the intervine voltage. The results obtained with N^+ and Ne^+ ions are shown in Fig. 4. At a same normalized intervine voltage, there should be theoretically no difference between the ions. Observed little discrepancies are probably due to imperfection in the input-beam emittances or an error in the intervine-voltage measurement or both.

Transmission efficiency

We measured the transmission efficiency as a function of the normalized intervine voltage. The transmission efficiency is defined by the ratio of the current of accelerated ions to that of the injected ions. Figure 5 shows experimental results obtained with N_2^+ and N^+ ions, indicated by \bullet and \circ , respectively. For comparison, we plot the results of two computer simulations using the PARMTEQ code and its modified version; as will be detailed in the next section, the former assumes an ideal electric field, and the latter uses more actual one. The modified PARMTEQ predicts lower transmission efficiencies but closer to the measured values.

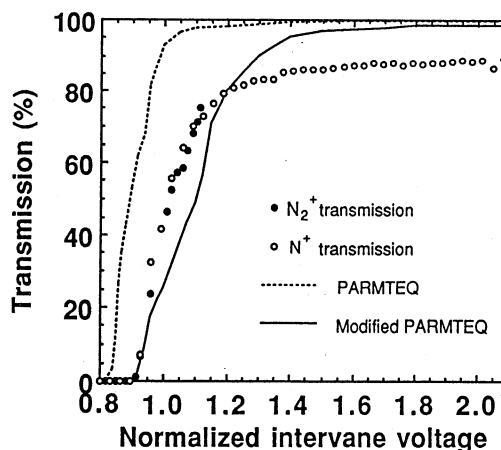


Figure 5. Transmission efficiencies as functions of the normalized intervine voltage. Experimental data obtained with N_2^+ and N^+ ions and two PARMTEQ predictions are plotted.

A₁₀ Effect

A and A₁₀ coefficients

In the commonly used PARMTEQ, the electric field is assumed to be the one derived from the two-term potential function:

$$U_2(r, \psi, z) = \frac{V}{2} \left[\left(\frac{r}{r_0} \right)^2 \cos 2\psi + AI_0(kr) \cos kz \right], \quad (1)$$

where V is the intervane voltage, $k = \pi/(\text{cell length})$, and I_0 is the modified Bessel function of order zero³. The parameters A and r_0 are determined by the boundary conditions:

$$A = \frac{m^2 - 1}{m^2 I_0(ka) + I_0(mka)}, \quad r_0 = a [1 - AI_0(ka)]^{-1/2}, \quad (2)$$

where a is the minimum distance from the z -axis to the vane tip, and ma is the maximum distance. Equating the right-hand side of Eq.(1) to $\pm V/2$, we have a equation representing equipotential surfaces. The ideal vanes would have surfaces same as the equipotential surfaces. For technical reasons, however, the geometry of actual vanes are different from that of the ideal ones, and therefore the actual electric field will be different from that used in the PARMTEQ simulation.

For the actual vanes, the potential function must be expressed in a general form:

$$U(r, \psi, z) = \frac{V}{2} \left[\sum_{i=1}^{\infty} A_{0i} r^{2i} \cos 2i\psi + \sum_{i=0}^{\infty} \sum_{j=1}^{\infty} A_{ji} I_{2i}(jkr) \cos 2i\psi \cos jkz \right]. \quad (3)$$

From the fourth symmetry condition, if i (j) is even, then j (i) must be odd. Using a program CHARGE 3-D, Crandall computed eight lowest order multipole coefficients for differing vane-tip geometries: the transverse radius of curvature (ρ_{\perp}) is variable with z or constant ($= r_0$ or $0.75r_0$); the longitudinal vane profile is standard (same as that of the ideal vanes) or sinusoidal⁴. He tabulates the resulting A_{ij} 's for an array of the modulation parameter m and the cell length divided by r_0 . At any geometry, the coefficients, except for A_{10} 's, are close to those of the two-term potential function, i.e., $A_{01}r_0^2$ is almost unity, and higher order terms are so small that they would be negligible. The A_{10} coefficient is, however, appreciably smaller than A , particularly at short cell lengths and small modulations at constant- ρ_{\perp} vanes.

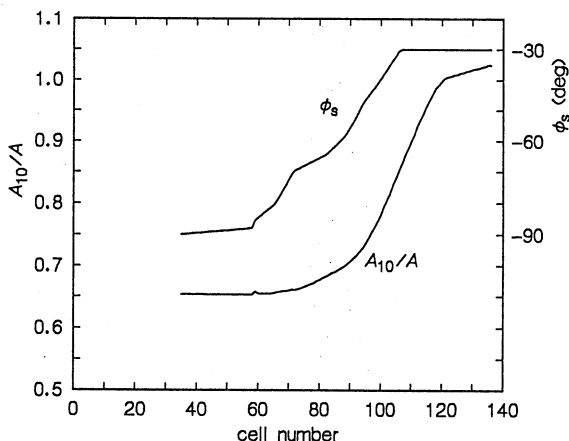


Figure 6. A_{10}/A ratio and the designed synchronous phase ϕ_s for the cells. The cells No.1 through 34 are for the radial matching section.

Modified PARMTEQ simulation

At our vanes, ρ_{\perp} is constant at $r_0 = 0.946$ cm, and the longitudinal vane tip profile is the standard one. We computed the A_{10}/A ratio for every cell by using an interpolation procedure on the table values; a computer program MOD12⁷ was used for the interpolation. The resulting A_{10}/A is shown in Fig. 6, along with the synchronous phase ϕ_s , the design values with $A_{10} = A$. The A_{10}/A ratio is smaller than unity in the bunching process, where synchronous phase increases from -90° to -30° . According to the PARMTEQ simulation with $A_{10} = A$, the ions are tightly packed in the separatrix during the bunching process. Since $A_{10} < A$, the separatrix shrinks both in width and height, and some ions will spill from the separatrix accordingly; as a result the transmission efficiency will be reduced.

In the simulation using the modified PARMTEQ, we use the above A_{10} in place of A . The resulting transmission efficiency follows fairly well the experimental data, as was shown in Fig. 5, though we have still discrepancy. The discrepancy is possibly due to that the A_{10} of the actual field in our RFQ is not exactly same as the Crandall's A_{10} , since the transverse cross section of our vanes may be different from that of the Crandall's model—the vane tip radius is same, but the width and height will be different. We will hence do the A_{10} computation for our vane geometry.

Acknowledgments

The authors express their thanks to M. Kihara (KEK) for his encouragement. Discussions with J. Staples (LBL) and S. Yamada (NIRS) have been valuable since the beginning of the A_{10} work. The RFQ development is supported by the Accelerator Research Division, High Energy Physics Division, and Nuclear Physics Division of INS, and by the Grant for Scientific Research of the Ministry Education, Science and Culture. The computer works were done on FACOM M780 in the INS Computer Room.

References

1. N. Tokuda *et al.*, *Structure and RF Characteristics of the INS 25.5-MHz Split Coaxial RFQ*, 7th Symp. on Acc. Sci. and Tech., Osaka, Japan, Dec., 1989.
2. S. Shibuya *et al.*, *RF Tests on the INS 25.5-MHz Split Coaxial RFQ*, 1990 Linear Acc. Conf., Albuquerque, NM, U.S.A., Sept., 1990.
3. K. R. Crandall *et al.*, *RF Quadrupole Beam Dynamics Design Studies*, 1979 Linear Accelerator Conference, Montauk, NY, U.S.A., March, 1979.
4. K. R. Crandall, *Effects of Vane-Tip Geometry on the Electric Fields in Radio-Frequency Quadrupole Linacs*, Los Alamos Technical Report, LA-9695-MS, 1983.
5. S. Arai *et al.*, *Acceleration Tests of the INS 25.5-MHz Split Coaxial RFQ*, IEEE 1991 Particle Acc. Conf., San Francisco, CA, U.S.A., May, 1991.
6. E. Tojyo *et al.*, *Development of the Compact ECR Ion Source for Injection to the INS SCRFQ Linac*, 14th Symp. on Ion Sources and Ion-Assisted Tech., Tokyo, Japan, June, 1991.
7. J. Staples, Private communication.